European Review for Medical and Pharmacological Sciences 2016; 20: 1923-1933

Analysis of nasal cavity morphology and nasolabial development of the normal Han ethnic people under age of 12

L. LI, W.-S. LI, Y.-U. LI, L.-S. LIAO, Y.-T. LIU, L. LI

Stomatology Department of Children's Hospital of Chongqing Medical University, Chongqing, China

Abstract. – OBJECTIVE: This study aims to establish the three-dimensional (3D) reconstruction model of nasal cavity for China's Han ethnic population (0-12 years) by laser scanning and photogrammetry, and thus to elucidate the developmental mechanism of nasal cavity morphology and nasolabial region.

PATIENTS AND METHODS: A total of 260 normal people of the Han ethnic aged 0-12 were recruited as subjects, among whom 60 were scanned for nasal cavity morphology in order to get reconstructed models with the computer engineering software. Photogrammetry was performed for the remaining 200 subjects to measure the 7 parameters that reflect vertically or horizontally the anatomical features of the nasolabial region.

RESULTS: The interior morphology of nasal cavity was accurately established by 3D laser scanning and photogrammetry with the optimal morphology of nasal cavity simulated through 3D reconstruction. Development of nasal cavity and nasolabial region was also analyzed.

CONCLUSIONS: The 3D laser scanning analysis is the ideal method to analyze the interior morphology of nasal cavity by reconstructing the normal interior morphology of nasal cavity and quantitatively analyze the change of nasal cavity morphology with age. Photogrammetry can be applied to conduct the morphological measurement for the nasolabial region and, thus, assessing the development of the nasolabial region with age, which provides information for choosing the timing and options of surgery in treating harelip and nasal deformity.

Key Words:
Laser scanning, Nasal cavity, Photogrammetry, Nasolabial development.

Introduction

Harelip is a common congenital oral and maxillofacial malformation and is always accompanied with nasal deformity regardless of severity. Nasal deformity affecting facial appearance remains even after proper cheiloplasty. In clinical practice, the bionic nose made by silicone rubber is usually placed in the nasal cavity, which effectively minimizes the effects of cicatricial contraction and plasticity and memorability of deformed cartilage on nasal appearance.

However, morphological characteristics of the nasal region differ somehow among different ethnic groups[1,2]. Currently, Chinese patients are mainly planted with bionic nose models originally designed for western population, which may not necessarily fit. Moreover, these bionic nose models are in a cylinder shape and cannot accurately simulate the nasal cavity morphology. Previously, several studies[3,4] have discussed the relationship between the nasal development and facial soft tissues, which, however, failed to describe the interior morphology of nasal cavity, or the development of nasal cavity and nasolabial region.

This study aims to conduct perform morphological measurements of the nasolabial region with photogrammetry for normal Han ethnic people aged 0-12 years based on 3D laser scanning and reconstitution of nasal cavity models, in hope to obtain the characteristics of normal nasal cavity and nasolabial region from each age group, and elucidate the development of nasal cavity and nasolabial region with age. Furthermore, the specialized bionic nose model may provide useful information for timing and options of surgery treating harelip and nasal deformity.

Patients and Methods

Patients

From February 2010 to October 2012, 260 patients of the Han ethnic (0-12 years old), who came to the Stomatology Department of Chil-

Corresponding Author: Wanshan Li, MD; e-mail: li¬¬¬¬_wanshanal@163.com

dren's Hospital of Chongqing Medical University due to unrelated sickness, were enrolled in this study. A cohort of 60 patients was investigated by the laser scanning and the remaining 200 patients by the photogrammetry. Then patients were divided into 10 age subgroups with male to female ratio in each group controlled around 1:1. The inclusion criteria are briefly described as follows. People of the Han ethnic, under the age of 12 years old with a normal nasal cavity and facial development and no skull illness; complete teeth and normal occlusal relation; without other known trauma and previous orthodontic treatment.

Laser Scanning Cohort

Model Preparation and Perfusion

Before treatment, all subjects were comprehensively assessed to exclude any organic diseases that may affect the model preparation and, thus, ensured the safety of subjects[5]. After general anesthesia, the nasal cavity model was obtained with the alginate materials with subjects in the supine position. The alginate materials were uniformly mixed into the nasal cavity (filling the vestibulum nasi up to the limen nasi), and removed after the materials solidified. The die stone model was used, and the whole process was similar to previously described models. After the model had dried completely, the model was manufactured in 98% vacuum environment, and then was transferred into the 60°C oven. After 8 hours of baking, the model was completely prepared for laser scanning.

Model Scanning

The ATOS II laser scanner was used to scan the left and right side of nasal cavity respectively. Then, the data from both sides were integrated and automatically aligned in the unified coordinate system, which could display the 3D point clouds for further analysis.

Digital Model Establishment

The point cloud images of 6 models in each group were unified, and the section lines were drawn with an interval of 0.5 mm. Under the premise of ensuring model authenticity, the section lines with obvious deviation were eliminated. Then, the average point cloud data was obtained, and the nasal cavity models were reconstructed through triangularization.

Selection and Criteria of Measured Values

Data section and measurement were conducted with the software Unigraphics 8.5. For the reconstruction models, the outermost section of the nasal cavity was extracted as the reference plane and set as Plane 1, the first narrow section after entering the nasal cavity as Plane 2, the most inflated section in the nasal cavity as Plane 3, and the limen nasi section as Plane 4. The longest horizontal distance in each plane is set as Value a (width of the nasal cavity of this section), and the longest vertical distance is set as Value b (height of nasal cavity of this section). After measuring values a and b of the 4 planes, we obtained a1, a2, a3, a4, b1, b2, b3 and b4. Straight lines were drawn vertical to Plane 1 to Plane 2, 3 and 4, respectively, to get the distance (marked as C1, C2, C3, respectively). Specifically, C1 was the distance from the first narrow section to the outermost section; C2 was the distance from the most inflated section to the outermost section; C3 was the distance from the limen nasi section to the outermost section of the nasal cavity, which is also the length of the nasal cavity (Figure 1). The data collection was conducted for five times in total with an interval of 1-2 weeks.

Statistical Analysis for Laser Scanning Cohort

The statistical analysis was conducted with SPSS 18.0 (SPSS Inc., Chicago, IL, USA), and all values were expressed as mean ± standard errors. The paired t-test was applied to test for any potential significant difference in 4 planes of point cloud images and reconstruction models between age groups. Based on this analysis, whether 3D reconstruction models could accurately reflect the nasal cavity conditions of each subject was determined. One way ANOVA and Tukey HSD test was conducted to assess for any potential significant difference in the development of nasal cavity between age groups (Tables VI and VII). $p < 0.05$ was considered statistically significant.

Photogrammetry Cohort

Measurements of Mark Points in Nasolabial Region

Canon D600 digital camera was applied to shoot the facial anteroposterior (the distance between the camera and sagittal line of the subject was 1 m, with the center of lens focuses on the spex nasi), basis nasi (the subject faced the cam-

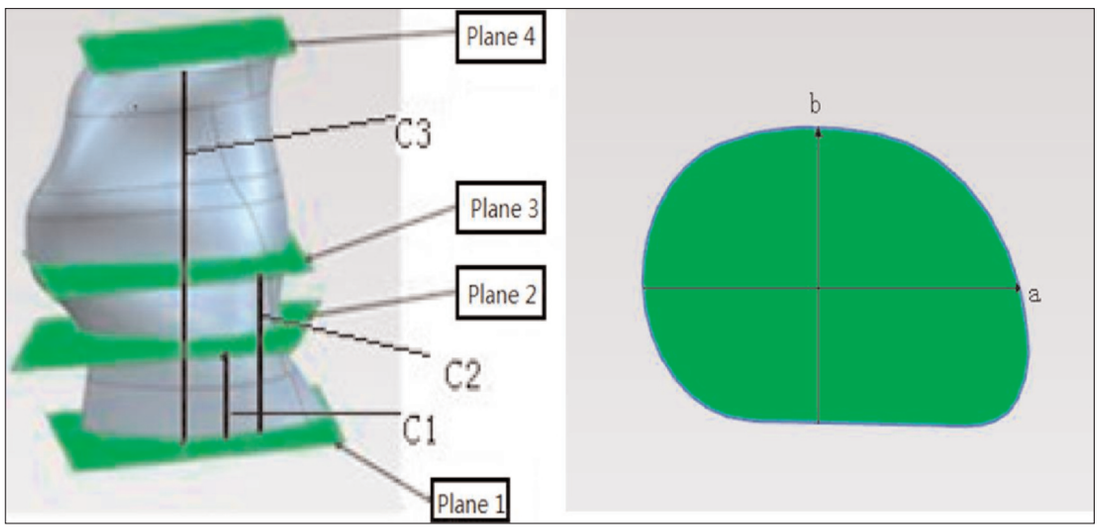

Figure 1. ***Left)*** The definition of the Planes and C values; ***Right)*** The definition of a and b values.

era, with the head bending backward to position the basis nasi horizontal with the weight cord, and the center of lens focused on the nostril base) and side pictures (the distance between the camera and sagittal line of the subject was 1 m, with the center of the lens focused on the middle of zygomatic arch)[6]. Before shooting, a 5 cm steel rule was used as a scale. During the shooting process, the subjects were required to look straight ahead with the eye-ear plane in parallel with the ground, and the lip naturally loosing and slightly close with rest bite. The shooting process should be consistent and finished successively. All the pictures were saved and appropriate ones were used for measurement of anatomical mark points. The image measurement analysis software Digimizer 4.0.0.0 (MedCalc Software, Florham Park, NJ, USA) was applied to mark the anatomical points[7] and measure both distance and angle. All results were further calibrated with a 5 cm steel ruler in the pictures (Figure 2). All measurements were repeated for 5 times with an interval of 2-3 weeks. The average number was used for statistical analysis. All shootings were completed by the same investigator to ensure consistent shooting process.

Statistical Analysis

Statistical analysis was performed with SPSS 18.0 (SPSS Inc., Chicago, IL, USA). The average number of each parameter of the nasolabial region is expressed as mean ± standard errors. One-way ANOVA and Tukey HSD test were conducted for any potential significant difference among age groups. $p < 0.05$ was considered statistically significant.

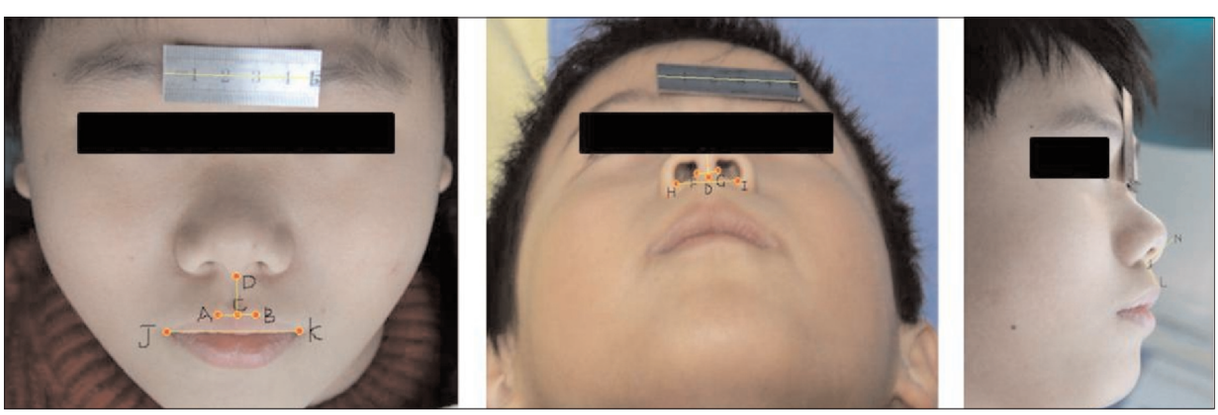

Figure 2. ***Left)*** Anteroposterior; middle) Nose bottom; ***Right)*** Lateral side.

Laser Scanner Equipment and Software Installed

ATOS II 3D scanner (GOM Company, Herzogenaurach, Germany) was applied, which can clearly detect the subtle features with a density of point cloud < 0.02 mm, and it is PTB proven with a measurement precision of < 0.1 mm/m, which meets the requirements of VDI/VDE 2634. Computer installed with Intel Pentium IV 2140GHz, Windows XP operating system, and Unigraphics NX 8.5 (Siemens PLM Software, Linz, Germany) were used in this study.

Results

Growth of Heights, widths and Lengths of nasal Cavity with Age

The measured parameters of the reconstruction models and point cloud images included width, height and length of the nasal cavity. These results showed that the measured parameters (width, height, length) were comparable between the reconstructed models and point cloud images (Tables I to IV). The heights, widths and lengths of nasal cavity at different time-points were measured and their growths with age were determined (Figures 3-5). As shown in Figure 3, the growth of widths in the period of 0 to 6 months and 1.5 to 4 years were relatively slow. A similar pattern was observed in the growth of length of the nasal cavity (Figure 5). From 0 to 1 year and 4 to 6 years, a rapid growth of heights of the nasal cavity was observed (Figure 4). Since these results were consistent with other publications, the 3D reconstruction models of nasal cavity were considered accurate enough to represent the average levels of all subjects within the group, and simulate the nasal cavity morphology from each age subgroup.

Growth of Widths, Heights, Nasolabial Angles of Nasolabial Region with Age

The corresponding parameters of nasolabial development at different time-points were measured (Table V) as well as the growths with age (Figures 6 to 8). As shown in Figure 6, the widths of upper lip were growing rapidly from 0 to 1 year and 4 to 6 years. Similarly, the heights of upper lip grow rapidly from 3 to 6 months and 4 to 6 years of age. Heights of nose grew rapidly from 6 months to 2 years and 4 to 6 years, while widths of nose grow relatively slow. These results consistent with previous literature indicated that the growth patterns of different regions were distinct.

Discussion

Reliability of 3D Laser Scanning Technology

Three-dimensional laser scanning technology is a tool that is germane to the exploration of a wide variety of research areas encompassing science, engineering, medicine, physical therapy and even fashion. Currently, the 3D laser scanning technology is one of the most advanced measurement technology for the human body or of certain anatomical areas has gained an ever in-

Table I. The average values and the results of the paired *t*-test for nasal cavity widths of the reconstruction models and point cloud images.

a		0-3m	3-6m	6-12m	1-1.5y	1.5-2y	2-3y	3-4y	4-6y	6-9y	9-12y
a1	N	6.49 ± 0.01	6.66 ± 0.01	7.00 ± 0.01	7.19 ± 0.01	7.33 ± 0.01	7.4 ± 0.01	7.72 ± 0.02	8.47 ± 0.02	8.53 ± 0.02	9.36 ± 0.09
	S	6.51 ± 0.19	6.50 ± 0.84	7.28 ± 0.23	6.86 ± 0.24	7.13 ± 0.21	7.01 ± 0.42	7.95 ± 0.76	8.55 ± 0.61	8.47 ± 0.31	9.62 ± 0.87
	P	0.882	0.753	0.109	0.662	0.171	0.196	0.686	0.778	0.874	0.587
a2	N	5.44 ± 0.01	6.04 ± 0.01	6.74 ± 0.01	6.86 ± 0.01	7.1 ± 0.01	7.28 ± 0.01	7.47 ± 0.02	8.52 ± 0.01	8.43 ± 0.02	9.22 ± 0.02
	S	5.35 ± 0.23	6.06 ± 0.69	6.99 ± 0.22	6.58 ± 0.24	6.86 ± 0.25	6.81 ± 0.47	7.58 ± 0.77	8.37 ± 0.65	8.33 ± 0.32	9.44 ± 0.85
	P	0.719	0.356	0.089	0.579	0.15	0.161	0.821	0.791	0.526	0.699
a3	N	6.68 ± 0.01	6.63 ± 0.01	7.60 ± 0.01	7.59 ± 0.01	8.63 ± 0.01	8.54 ± 0.02	8.88 ± 0.02	9.24 ± 0.01	9.42 ± 0.02	10.35 ± 0.02
	S	6.58 ± 0.39	6.47 ± 0.82	7.74 ± 0.26	7.36 ± 0.26	8.37 ± 0.24	8.13 ± 0.44	9.01 ± 0.78	9.15 ± 0.61	9.32 ± 0.32	10.54 ± 0.83
	P	0.846	0.867	0.127	0.844	0.092	0.2	0.848	0.927	0.581	0.781
a4	N	4.84 ± 0.01	6.43 ± 0.01	7.12 ± 0.01	7.33 ± 0.01	9.19 ± 0.01	9.1 ± 0.01	9.28 ± 0.01	9.03 ± 0.02	8.97 ± 0.01	8.46 ± 0.01
	S	4.75 ± 0.23	6.23 ± 0.79	7.23 ± 0.32	7.08 ± 0.25	8.91 ± 0.19	9.31 ± 0.18	9.44 ± 0.67	8.94 ± 0.59	8.31 ± 0.29	8.63 ± 0.81
	P	0.837	0.97	0.227	0.472	0.052	0.066	0.696	0.873	0.372	0.857

N, number of reconstruction models in each group; S, the average number of point cloud images of subjects in each group, in mm; m, months; y, years; P, *p* value (significant level of $\alpha = 0.05$).

Table II. The average values and the results of the paired t-test for nasal cavity heights of the reconstruction models and point cloud images.

b		0-3m	3-6m	6-12m	1-1.5y	1.5-2y	2-3y	3-4y	4-6y	6-9y	9-12y
b1	N	3.88 ± 0.01	4.71 ± 0.01	5.82 ± 0.01	5.88 ± 0.02	5.94 ± 0.01	6.07 ± 0.02	6.62 ± 0.02	7.47 ± 0.02	7.62 ± 0.02	7.74 ± 0.03
	S	3.92 ± 0.16	5.12 ± 0.34	5.91 ± 0.43	6.19 ± 0.40	5.65 ± 0.31	5.83 ± 0.41	6.26 ± 0.40	7.21 ± 0.52	7.53 ± 0.31	7.49 ± 0.48
	P	0.696	0.141	0.374	0.086	0.772	0.514	0.245	0.565	0.834	0.426
b2	N	3.4 ± 0.01	4.25 ± 0.02	4.24 ± 0.01	5.85 ± 0.01	5.87 ± 0.01	5.78 ± 0.01	5.36 ± 0.03	6.8 ± 0.01	7.31 ± 0.01	7.38 ± 0.01
	S	3.49 ± 0.18	4.6 ± 0.19	4.46 ± 0.41	6.22 ± 0.39	5.83 ± 0.79	5.96 ± 0.23	5.34 ± 0.42	6.99 ± 0.34	7.27 ± 0.32	7.39 ± 0.51
	P	0.376	0.051	0.148	0.126	0.913	0.077	0.829	0.265	0.538	0.553
b3	N	3.53 ± 0.01	4.78 ± 0.01	4.76 ± 0.01	4.84 ± 0.01	4.86 ± 0.01	4.88 ± 0.02	5.78 ± 0.02	6.27 ± 0.02	7.32 ± 0.02	7.46 ± 0.01
	S	3.58 ± 0.16	4.89 ± 0.37	4.89 ± 0.39	5.20 ± 0.39	4.82 ± 0.73	4.87 ± 0.24	5.80 ± 0.44	6.40 ± 0.36	7.25 ± 0.32	7.61 ± 0.48
	P	0.51	0.661	0.864	0.063	0.885	0.3	0.863	0.397	0.76	0.537
b4	N	3.61 ± 0.01	3.68 ± 0.02	4.35 ± 0.01	4.89 ± 0.01	4.89 ± 0.02	5.53 ± 0.01	5.7 ± 0.02	6.67 ± 0.02	7.05 ± 0.03	7.37 ± 0.02
	S	3.68 ± 0.16	3.83 ± 0.27	4.64 ± 0.39	5.21 ± 0.35	4.80 ± 0.76	5.68 ± 0.23	5.59 ± 0.42	6.84 ± 0.33	7.97 ± 0.32	7.72 ± 0.48
	P	0.448	0.314	0.063	0.06	0.986	0.615	0.675	0.303	0.961	0.489

N, number of reconstruction models in each group; S, the average number of point cloud images of subjects in each group, in mm; m, months; y, years; P, *p* value (significant level of $\alpha = 0.05$).

Table III. The average values and the results of the paired t-test for nasal cavity lengths of the reconstruction models and point cloud images.

C		0-3m	3-6m	6-12m	1-1.5y	1.5-2y	2-3y	3-4y	4-6y	6-9y	9-12y
C1	N	2 ± 0	1 ± 0	1 ± 0	1 ± 0	1 ± 0	1 ± 0	1.5 ± 0	1 ± 0	1 ± 0	1 ± 0
	S	1.92 ± 0.49	1.17 ± 0.26	1.17 ± 0.26	1.25 ± 0.27	1.17 ± 0.26	0.92 ± 0.2	1.67 ± 0.4	1.08 ± 0.38	1.08 ± 0.38	1.08 ± 0.38
	P	0.695	0.175	0.175	0.076	0.175	0.363	0.363	0.611	0.611	0.611
C2	N	3.5 ± 0	4 ± 0	3.5 ± 0	3 ± 0	4 ± 0	5 ± 0	4.5 ± 0	5.5 ± 0	6.5 ± 0	6.5 ± 0
	S	3.42 ± 0.49	3.92 ± 0.38	3.58 ± 0.38	3.08 ± 0.2	4.17 ± 0.26	4.92 ± 0.38	4.42 ± 0.49	5.25 ± 0.27	6.42 ± 0.38	6.42 ± 0.38
	P	0.695	0.611	0.611	0.363	0.175	0.611	0.695	0.076	0.611	0.611
C3	N	6 ± 0	6 ± 0	6.5 ± 0	7 ± 0	7.5 ± 0	7.5 ± 0	7.5 ± 0	8 ± 0	9 ± 0	9.5 ± 0
	S	5.75 ± 0.61	5.75 ± 0.61	6.41 ± 0.38	7.08 ± 0.38	7.33 ± 0.26	7.33 ± 0.26	7.25 ± 0.27	7.83 ± 0.26	8.92 ± 0.49	9.58 ± 0.2
	P	0.358	0.358	0.611	0.611	0.175	0.175	0.076	0.175	0.695	0.363

N, number of reconstruction models in each group; S, the average number of point cloud images of subjects in each group, in mm; m, months; y, years; P, *p* value (significant level of $\alpha = 0.05$).

Table IV. The results of Tukey HSD test.

Grouping	a1 T	a2 T	a3T	a4 T	b1 T	b2 T	b3 T	b4 T	C1 T	C2 T	C3 T
0-3m	d	d	d	d	d	d	d	d	d	d	d
3-6m	d	e	d	e	e	e	e	d	e	e	d
6-12m	e	f	e	e	f	f	e	e	e	d	e
1-1.5y	e	f	e	f	g	g	e	f	e	f	f
1.5-2y	e	f	f	g	g	g	e	f	e	e	g
2-3y	e	f	f	g	g	g	e	g	e	g	g
3-4y	f	g	g	g	h	h	f	h	f	h	g
4-6y	g	h	h	h	i	i	g	i	e	i	h
6-9y	g	h	h	h	i	j	h	j	e	j	i
9-12y	h	i	i	i	i	j	i	k	e	j	j

The same letters indicate no significant difference, and different letters indicate significant differences. T is the Tukey's interval obtained by the Tukey HSD test method.

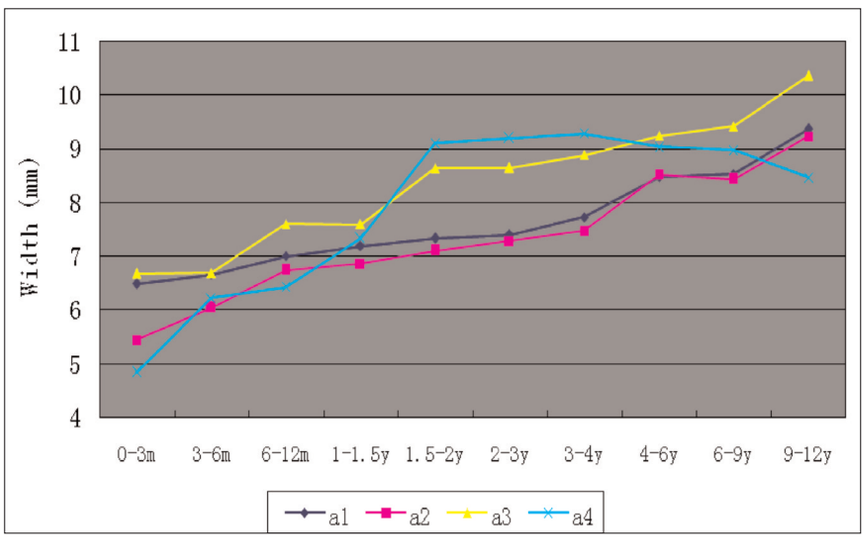

Figure 3. The change of nasal cavity widths with age.

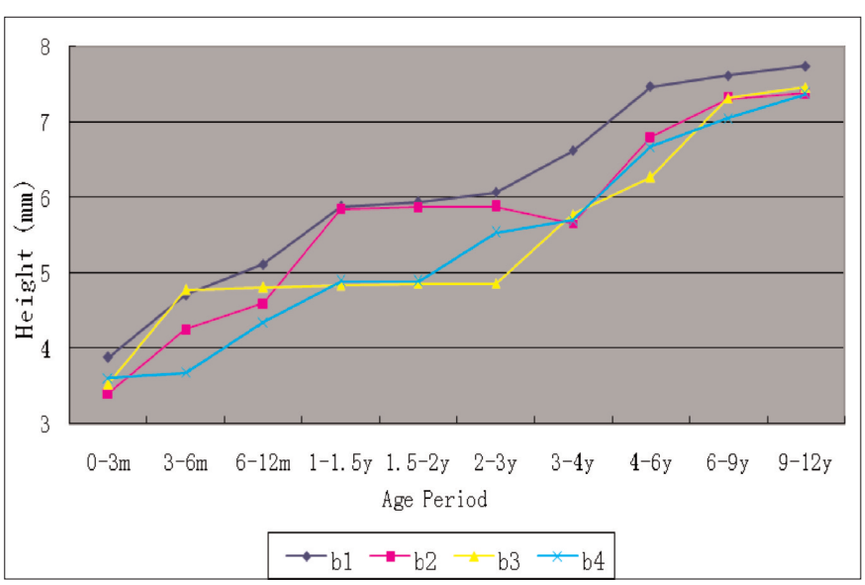

Figure 4. The change of nasal cavity heights with age.

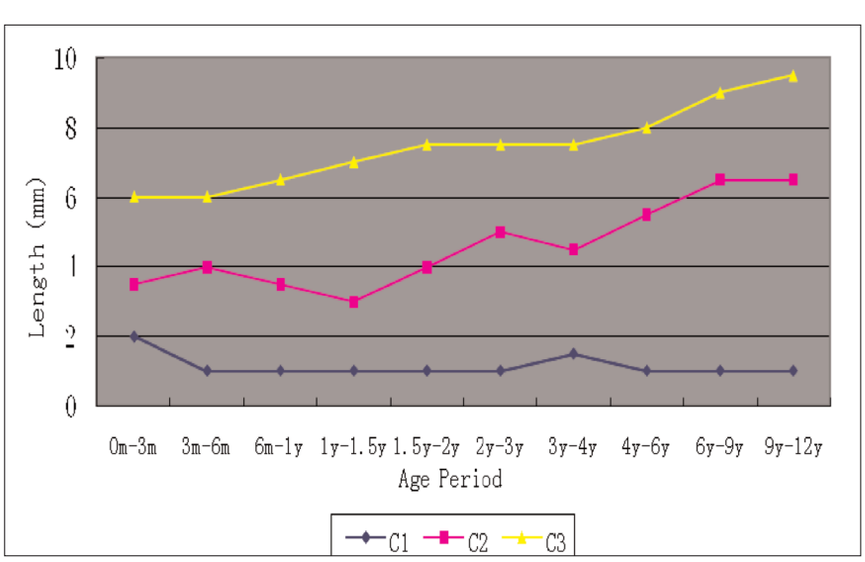

Figure 5. The change of nasal cavity lengths with age. C1, distance from the first narrow section to the outermost section; C2, distance from the most inflated section to the outermost section; C3, distance from the limen nasi section to the outermost section of the nasal cavity.

Table V. Measurements of nasolabial region.

Grouping	AB	CD	DE	FG	HI	JK	NL
0m-3m	4.90 ± 0.19	7.58 ± 0.32	5.38 ± 0.21	3.09 ± 0.12	12.78 ± 0.10	22.83 ± 0.74	103.61 ± 0.52
3m-6m	5.33 ± 0.16	8.21 ± 0.25	5.61 ± 0.18	3.85 ± 0.18	14.01 ± 0.51	24.73 ± 0.90	102.59 ± 0.49
6m-12m	5.76 ± 0.32	8.24 ± 0.34	5.95 ± 0.26	4.18 ± 0.20	15.44 ± 0.66	25.47 ± 0.95	100.99 ± 0.84
1y-1.5y	6.12 ± 0.12	8.24 ± 0.42	6.36 ± 0.21	4.61 ± 0.24	16.14 ± 0.27	27.54 ± 0.41	100.20 ± 0.86
1.5y-2y	6.56 ± 0.26	8.95 ± 0.30	6.90 ± 0.31	5.90 ± 0.50	16.81 ± 0.38	28.77 ± 0.58	98.48 ± 0.35
2y-3y	7.12 ± 0.29	9.22 ± 0.51	7.44 ± 0.18	5.78 ± 0.30	17.32 ± 0.36	30.16 ± 0.69	97.01 ± 0.48
3y-4y	7.40 ± 0.39	9.55 ± 0.55	8.97 ± 0.66	6.06 ± 0.21	17.79 ± 0.26	32.22 ± 1.19	96.48 ± 1.54
4y-6y	8.17 ± 0.24	12.07 ± 0.50	11.39 ± 0.67	6.50 ± 0.22	18.95 ± 0.65	36.45 ± 0.99	95.15 ± 1.10
6y-9y	8.63 ± 0.38	12.51 ± 0.73	11.72 ± 0.44	6.71 ± 0.26	21.02 ± 0.67	37.53 ± 1.21	93.97 ± 0.68
9y-12y	9.39 ± 0.30	13.29 ± 0.31	12.45 ± 0.36	7.05 ± 0.31	22.15 ± 0.75	39.89 ± 1.05	93.05 ± 0.58

AB, distance of bilateral cleft lips; CD, length of philtrum; DE, height of apex nasi; FG, width of columella nasi; HI, width of basis nasi; JK, distance of corner of the mouth; NL, nasolabial angle. The unit of NL is degree, and all other units are mm.

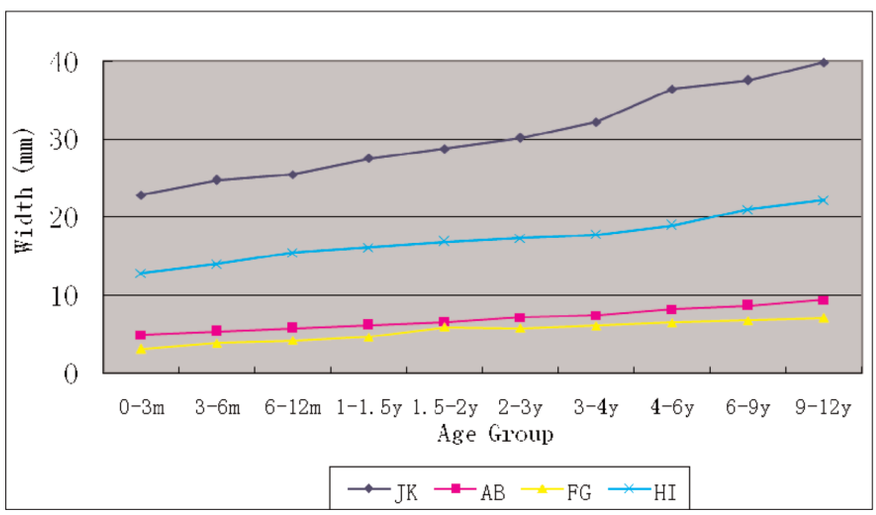

Figure 6. The change of widths of nasolabial region with age. AB, distance of bilateral cleft lips; FG, width of columella nasi; HI, width of basis nasi; JK, distance of corner of the mouth; NL, nasolabial angle.

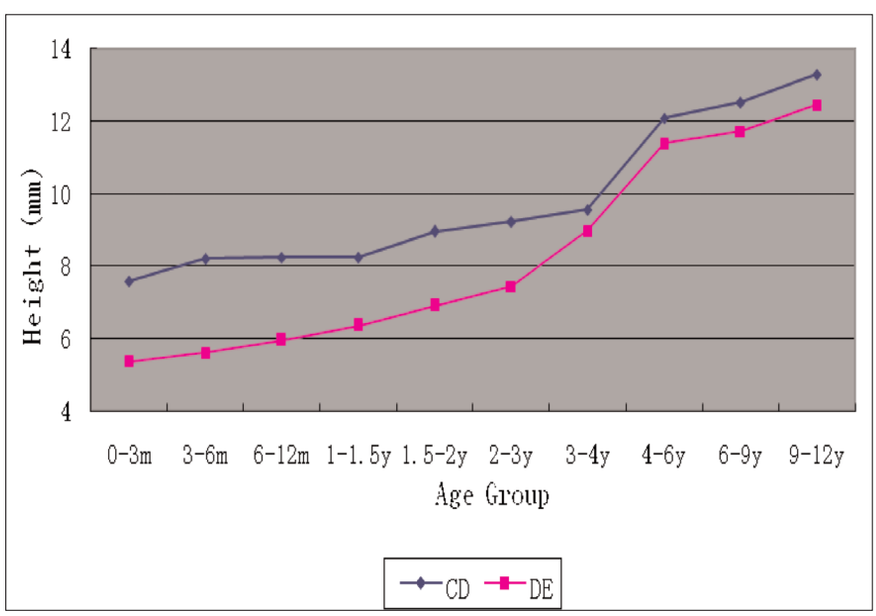

Figure 7. The change of heights of nasolabial region with age. CD, length of philtrum; DE, height of apex nasi.

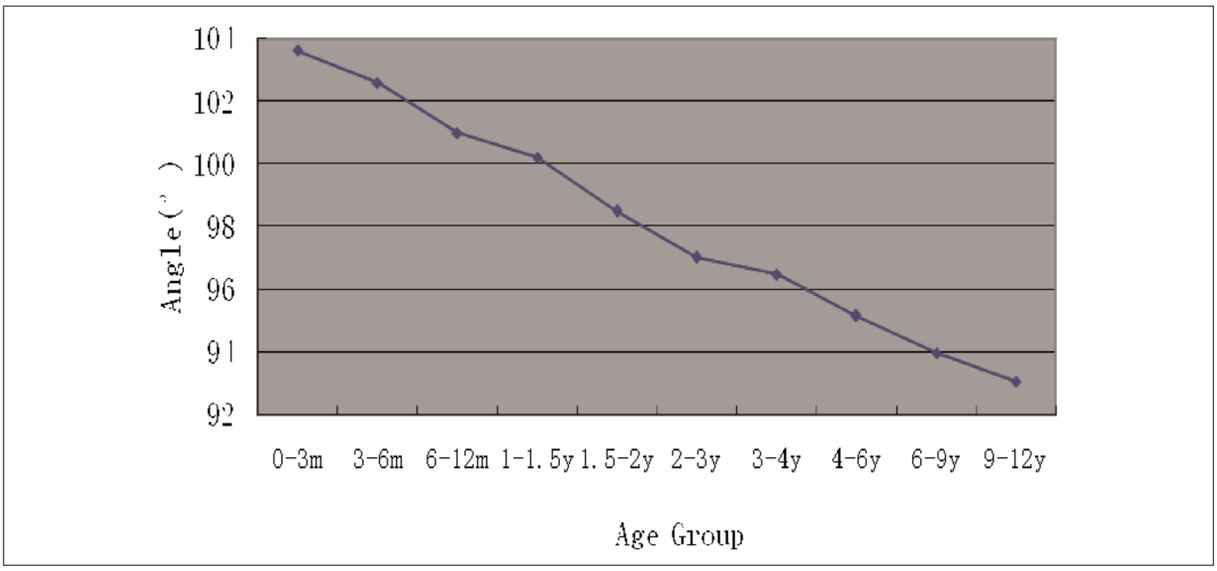

Figure 8. The change of angles of nasolabial region with age.

creasing importance in recent years, especially for soft tissue[8]. The measured results of soft tissue in maxillofacial region are better than the direct measurements. This technology is featured with advantages as non-invasion, no radiation, no pathogenicity, objectivity, repeatability, high precision and efficiency. The feasibility and reliability of this technology in the measurement of the nasal region have already been demonstrated (9,10). Moreover, the 3D laser scanning is performed without immediate contact, which is particularly appropriate for children.

ATOS II laser scanner used in this study is primarily composed of Fringe projection system and two CCD Cameras. Its working principle is similar to human eyes: with raster projection on the subject, the 3D features of subjects were obtained through processing digital images by the computer. With different models of measuring heads, a single measurement can collect up 800,000 to 4,000,000 points from the images. After calculating out the single measurement, with positioning by mark points and automatic computation, the actual morphology of subjects were obtained from the integration of all point cloud, and exported into STL files. Both cameras have calibration and self-monitoring functions to ensure the precision up to 0.1 mm/m, which meets the requirements of clinical practice.

Model Preparation, Nasal Cavity Morphology and Development

In this study, only Han ethnic (0-12 years old) were recruited as subjects, including some in-

Table VI. The results of one-way ANOVA.

Dependent variable	df	F	sig
AB	9	281.622	.000
CD	9	213.224	.000
DE	9	487.199	.000
FG	9	240.149	.000
HI	9	333.097	.000
JK	9	413.549	.000
NL	9	196.478	.000

AB, distance of bilateral cleft lips; CD, length of philtrum; DE, height of apex nasi; FG, width of columella nasi; HI, width of basis nasi; JK, distance of corner of the mouth; NL, nasolabial angle; df, the degree of freedom.

Table VII. The results of Tukey HSD test.

Grouping	AB T	CD T	DE T	FG T	HI T	JK T	NL T
0m-3m	a	a	a	a	a	a	a
3m-6m	b	b	a	b	b	b	a
6m-12m	c	b	b	B	c	b	b
1y-1.5y	c	b	c	C	c	c	b
1.5y-2y	d	c	d	D	d	c	c
2y-3y	e	c	e	D	e	d	d
3y-4y	e	c	f	D	f	e	d
4y-6y	f	d	g	E	g	f	e
6y-9y	g	d	g	E	h	f	f
9y-12y	h	e	h	F	i	g	f

AB, distance of bilateral cleft lips; CD, length of philtrum; DE, height of apex nasi; FG, width of columella nasi; HI, width of basis nasi; JK, distance of corner of the mouth; NL, nasolabial angle. The same letters mean no significant differences, different letters mean significant differences. T means the Tukey's interval obtained by the Tukey HSD test method.

fants who have weak tolerance. Also, great mobility with nasolabial region brings a further difficulty to accurate measurement since any discomfort may result in mobility of local organs. Furthermore, it takes a relatively long time to obtain models of the nasal cavity. Therefore, to ensure the accuracy of models, all subjects were under general anesthesia during the modeling process. However, it should be noted that patients were not put anesthesia only due to collecting experiment data, but also for treatment of other oral cavity diseases, which would not increase additional economic or physiological burden for patients. To ensure the precision, the modeling materials should be with moderate viscosity, bubbles and local tissue deformation should be avoided by operating gently. Besides, timely model modeling should be performed to avoid the potential deformation of models. To avoid potential deformation and bubbles, when duplicating the mold, it should be conducted in the 98% vacuum environment after the model is completely dry.

From the reconstruction models established in our study, the interior morphology of nasal cavity is not in cylinder shape as clinically used nose models, but of column shape with narrow and inflated parts. The width, height and length of the nasal cavity increases with age, however, with varying growth speed in different age periods. From 0 to 6 months and 1.5 to 4 years, the growth in length and width is slower, while, from 0 to 1 year old and 4 to 6 years, remarkable growth in height was observed. These results are consistent with a previous report[11,12]. It indicated that the 3D reconstruction models of nasal cavity from each age group were accurate enough to represent the general conditions of subjects, and satisfactorily simulate the nasal cavity morphology of each age subgroup.

Mechanism of Nasolabial Region Development

The width of upper lip increases rapidly from 0 to 1 year and 4 to 6 years. The height of upper lip increases rapidly from 3 to 6 months and 4 to 6 years old. The height of nose increases quickly from 6 months to 2 years and 4 to 6 years, while the width of nose increases relatively slowly. These results are consistent with data previously reported[13,14]. In addition, this research indicated that the growth of width and height of upper lip and height of nose are uneven and have their own rapid growing phase, while the growth of the nasolabial region is generally even. These results agreed with previous literature and indicated that the growth pattern of different regions was distinct.

Morphological Measurements and Quantitative Analysis

The morphological measurements of the face have been studied for a long history, with relevant records reported as early as from ancient Greece and Egypt (15). The history of morphological measurements is a history towards better precision. Until now, a huge gap of morphological measurements of the nasolabial region remains between manual measurement and automatic modeling, measurement and analysis, and from slow and error-prone measurement with direct contact to accurate measurement without di-

rect contacts. With the development of computer science during recent years, optics and graphics, digital images become the main approach to obtain substantial valuable information[16]. Therefore, measurement of facial soft tissue with digital images becomes a novel method which does not require expensive equipment and complicated collection process of graphs. All it needs is a normal digital camera and a computer equipped with relevant hardware. With the processing of 2D digital images with software, facial measurement analysis can be realized in a simple, fast, accurate, non-contact and repeatable manner.

In this study, Digimizer 4.0.0.0 software was used to measure and analyze the images after manually positioning the anatomical mark points in facial anteroposterior, basis nasi and lateral digital images. Meanwhile, prior to shooting the pictures, a 5 cm steel ruler was used as the scale to rectify the measurements. Farkas et al[17] proposed the method for human body measurement and photogrammetry, and identified 11 reliable mark points for soft tissue including apex nasi point, subnasal point, mouth corner point, upper lip salient point and lower lip salient point. Bearn et al[18] discussed the remarkable repeatability of angle measurements and concluded that soft tissue profile analysis from photographs can be regarded as reliable and robust under a range of conditions. Meanwhile, Becker et al[19] demonstrated the repeatability and consistency of photogrammetry by showing the similarity among results with 3 measurements and results achieved by 10 observers with a software program for 'on screen' image analysis. To minimize potential bias, 5 measurements were conducted for each time. Besides, to limit the systemic errors to 5%, all image shooting, identification of mark points and parameter measurements were conducted by the same researcher.

It is always a baffling issue about how to better analyze and compare the models quantitatively between different studies. Several studies conducted 2D or 3D analysis[20-21]. Seckel et al[20] tested the precision of landmark positioning for a set of landmarks that can be used for the edentulous cleft lip and palate maxilla of the infant, by analyzing intraobserver and interobserver repositioning and measuring on a series of 121 study casts, and a learning effect for precise positioning has been demonstrated in both analyses. However, the 2D analysis is insufficient for a 3D model of the nasal cavity with polymorphic transformation. The software Unigraphics NX 8.5 is produced by Siemens PLM Software Company based on the OpenGL software of 3D CAD/CAM/CAE, which provides the digital modeling and verification method for product design and manufacturing. In this study, we used this software to compare the interior morphological change of nasal cavity after model reconstruction. By measuring a, b, c values of the four planes in each group, the change of length, width and height of nasal cavity can be shown directly, which provides a solid foundation for further analysis of the periodical development of nasal cavity.

Conclusions

This technique reliably discriminates geometric features of craniofacial morphology that are associated with aspects of nose morphology. This study shows that the 3D laser scanning analysis is the ideal method to analyze the interior morphology of nasal cavity by reconstructing the normal interior morphology of nasal cavity in each age group, and quantitatively analyzing the growth pattern of nasal cavity morphology. Based on the mark points, the photogrammetry can be applied to measure for morphological traits of the nasolabial region, and thus assess its growth pattern, which provides information for choosing the timing and options of surgery in treating harelip and nasal deformity.

Conflict of Interest

The Authors declare that there are no conflicts of interest.

References

1) Milgrim LM, Lawson W, Cohen AF. Anthropometric analysis of the female Latino nose, Revised aesthetic concepts and their surgical implications. Arch Otolaryngol Head Neck Surg 1996; 122: 1079-1086.

2) Leong SC, White PS. A comparison of aesthetic proportions between the oriental and Caucasian nose. Clin Otolaryngol Allied Sci 2004; 29: 672-676.

3) Stephan CN, Henneberg M, Sampson W. Predicting nose projection and pronasal position in facial approximation: a test of published methods and proposal of new guidelines. Am J Phys Anthropol 2003; 122: 240-250.

4) Gulsen A, Okay C, Aslan BI, Uner O, Yavuzer R. The relationship between craniofacial structures

and the nose in Anatolian Turkish adults a cephalometric evaluation. Am J Orthod Dentofacial Orthop 2006; 130: 131.

5) Aminpour S, Tollefson TT. Recent advances in presurgical molding in cleft lip and palate. Curr Opin Otolaryngol Head Neck Surg 2008; 16: 339-346.

6) Zhang B, Li K, Xia C. Research on the morphology of 360 cases of normal Han nationality nose region among 0-6 years old and meanings. Shandong Medicine 2008; 48: 63-64.

7) Losee JE, Kirschner RE. Comprehensive Cleft Care. McGraw-Hill Medical 2008; 14: 198.

8) Bai Y, Guo H. 3D Reconstitution and measurement research development of skull facial soft tissue morphology. Foreign Medical Science Oral Cavity Fascicle 2007; 27: 220-222.

9) Liu X, Zhao Y, Wu G. Research on the reliability of 3d laser scanning measurement on external nose morphology. Pract Oral Med 2004; 20: 211-213.

10) Proff P, Weingärtner J, Rottner K, Bayerlein T, Schoebel S, Kaduk W, Gedrange T. Functional 3-D analysis of patients with unilateral cleft of lip.alveplus and pale (UCLAP) Following lip repair. J Craniomaxillofac Surg 2006; 34 Suppl 2: 26-30.

11) Pan S, Pan S. Research on the normal occlusion of children's skull facial development features in Shandong Province. Shandong University, 2009.

12) Egbert H, Huizing MD, John AM, Groot MD. Funct Reconstr Nasal Surg 2006; 1: 40-42.

13) Zhang B, Li K, Xia C. Research on the morphology of 360 cases of normal han nationality nose region among 0-6 years old and meanings. Shandong Medicine 2008; 48: 63-64.

14) Zhao Y, Wang Y, Wei X. Survey on 5-17 years old children's nasal part development in four Province. Pract Prevent Med 2001; 8: 90-91.

15) Vegter F, Hage JJ. Clinical anthropometry and canons of the face in historical perspective. Plast Reconstr Surg 2000; 106:1090-1096.

16) Fan Q, Li J. Research and realization on pictures' 3D human body models. Microcomputer Application 2006; 22: 5-6.

17) Farkas LG, Bryson W, Klotz J. Is photogrammetry of the face reliable? Plast Reconstr Surg 1980; 66: 346-355.

18) Bearn DR, Sandy JR, Shaw WC. Photogrammetric assessment of the soft tissue morphology in unilateral clef lip and palate. Cleft Palate Craniofac J 2002; 39: 597-603.

19) Becker M, Svensson H. Morphometry in digital photographs: a promising technique for assessing patients with cleft lip and palate. Scand J Plast Reconstr Surg Hand Surg 1998; 32: 295-299.

20) Seckel NG, van der Tweel I, Elema GA, Specken TF. Land mark positioning on maxilla of cleft lip and palate infant-a reality? Cleft Palate Craniofac J 1995; 32: 434-441.

21) Kriens O. Data objective diagnosis of infant cleft lip, alveolys and palate Morphologic data guiding understanding and treatment concepts. Cleft Palate Craniofac J 1991; 28: 157-168.